MOL2NET, 2023, 9, ISSN: 2624-5078
https://mol2net-09.sciforum.net/

MOL2NET'23, Conference on Molecular, Biomedical, Computational, & Network Science and Engineering, 8th ed.

Poinsettifolin A: virtual screening of flavonoids through molecular docking, dynamics, and MM/PBSA studies identify the compound as a potential NLRP3 inflammasome inhibitor.

Fernanda de França Genuíno Ramos Campos[a,b], Karla Joane da Silva Menezes[a,c], Washley Phyama de Jesus Marinho[a,b], Ricardo Olimpio de Moura, and Igor José dos Santos Nascimento[a,c].

[a] *Laboratory of Drug Synthesis and Development (LDSF), State University of Paraíba, Campina Grande-PB, Brazil.*

[b] *Pharmacy Department, Center for Biological and Health Sciences, State University of Paraíba, Campina Grande-PB, Brazil.*

[c] *Postgraduate Program in Pharmaceutical Sciences, State University of Paraíba, Campina Grande-PB, Brazil.*

** Corresponding Author: igorjsn@hotmail.com or igor.nascimento@cesmac.edu.br*

Graphical Abstract:

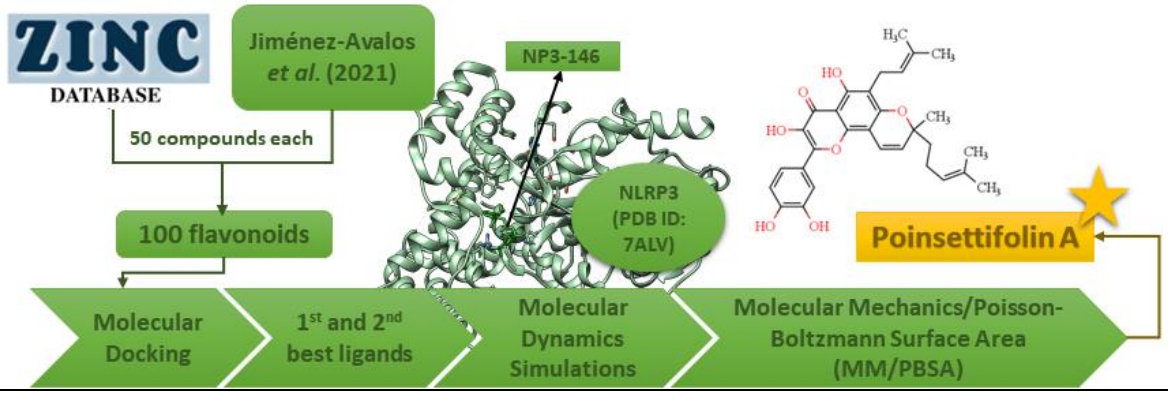

Abstract: Flavonoids are known to showcase anti-inflammatory abilities. Hence, it is not a wild guess that they might inhibit *NOD-, LRR- and pyrin domain-containing protein 3* (NLRP3) inflammasome signaling, implying these chemicals could inspire new drug candidates for this pathway. Thus, this work aims to identify flavonoids as potential NLRP3 inhibitors, using virtual screening of 100 known compounds through molecular docking, molecular dynamics, and MM/PBSA calculations. In this way, Dorsmanin C (DC) and Poinsettifolin A (PA) were the best compounds after molecular docking, binding to critical residue Arg^{578}, which is essential for activity. In MD simulations, PA provides the best stability at the binding site of the target, better than DC and NP3-146 (known inhibitor), demonstrated by RMSD, RMSF, R_g, and SASA plots. Next, MM/PBSA calculations provide the best binding energy for NP3-146 compared to PA and DC, yet PA still proves superior to DC regarding target affinity. Therefore, Poinsettifollin A is the most promising candidate, highlighting it as a potential lead for developing novel anti-inflammatory drugs targeting NLRP3.

1. Introduction

Inflammation is an organism's primary response as protection from infection or injury. In mammals, inflammation causes vasodilation and permeation of the vascular endothelium through the recruitment and activation of immune cells. The normal inflammatory response allows the removal of harmful stimuli and the restoration of homeostasis. However, exacerbated inflammation can lead to chronicity and harm the body [1,2]. The initiation of the inflammatory response depends on the recognition of pathogen-associated molecular patterns (PAMPs) and damage-associated molecular patterns (DAMPs) by pattern recognition receptors (PRRs), such as Toll-like receptors (TLRs) and Toll-like receptors (TLRs), such as the nucleotide-binding oligomerization domain (NLRs) [3].

Inflammasomes, innate immunity components, are macromolecules originating from inflammatory stimuli. Upon recognition of PAMPs and DAMPs, inflammasomes are activated within immune cells. The best-described inflammasome is the NOD-like receptor family containing pyrin domain 3 (NLRP3), which functions in innate immunity and mediates pathological conditions such as chronic inflammatory diseases [4,5]. Therefore, NLRP3 is an important target of inflammation, and recognizing its mechanisms is essential.

Among the compounds already reported anti-inflammatory activity are flavonoids, a class of secondary plant metabolites. Several mechanisms have been demonstrated for anti-inflammatory activity, such as inhibiting the enzyme cyclooxygenase-2 and lipoxygenases [6]. Furthermore, some flavonoids regulate the transcriptional expression of pro-inflammatory enzymes, such as inducible nitric oxide synthase, and pro-inflammatory cytokines, such as IL-1 and tumor necrosis factor-alpha (TNF-α). Transcriptional factors are also influenced by flavonoids, such as nuclear factor-κB (NF-κB) [7].

It is known that some flavonoids control the assembly of the NLRP3 inflammasome. Apigenin has in vitro activity preventing the oligomerization of NLRP3 [8,9], while quercetin, luteolin, and apigenin act to suppress NLRP3 and caspase-1 activation in human umbilical vein endothelial cells, and in vivo, with rat and mouse models [10-12]. Thus, it should be noted that flavonoids influence the NLRP3 inflammasome pathway.

Computer-aided drug design (CADD) is helpful because it is fast and inexpensive, combining several computational tools to identify and develop a lead compound. Molecular docking is the most used method, with which the binding mode of a compound to the target is obtained. In addition, Molecular Dynamics (MD) simulations provide the most accurate pose of the drug-target complex. CADD can be used to discover anti-inflammatory lead compounds [13,14].

Here, we identified flavonoids with the potential against NLRP3 through molecular docking for virtual screening of 100 known compounds identified as flavonoids, with subsequent analysis of MD simulation and MM/PBSA calculations. Therefore, Poinsettifollin A was the most promising candidate, highlighting it as a potential lead for developing novel anti-inflammatory drugs targeting NLRP3.

2. Material and Methods

2.1 Target and Ligand Selection

100 flavonoids were selected from the ZINC20 [15] database and others from the database published by Jiménez-Avalos and collaborators [16] (Supplementary Material). Conformational analysis of all ligands was performed using *MarvinSketch*® software. The lowest energy conformer obtained out of 10 had its conformation further refined by semi-empirical quantum mechanical energy minimization through Austin Model 1 (AM1) in ArgusLab® [17] software. At the same time, The structure of NLRP3 was obtained through a search on the UniProt website (www.uniprot.org) [18], obtained from the Research Collaboratory for Structural Bioinformatics Protein Data Bank database (RCSB.org) [19], under the code 7ALV [20].

2.2 Virtual screening protocol validation

Afterward, the method for virtual screening using molecular docking in the chosen structure was validated using *GOLD*® software [21]. All hydrogens were added, the co-crystallized ligand was removed, and redocking was performed in the four scoring functions (ChemPLP, GoldScore, ChemScore, and ASP) (Supplementary Material). This led to the lowest RMSD value of 0.549 Å obtained by the ChemScore function, chosen for docking assays. In addition, the Fit score value of 33.70 for the best pose was used as a starting point to select the best inhibitors for the MD simulations.

2.3 Molecular Dynamics Simulations

The best complexes after molecular docking were used Molecular Dynamics (MD) simulation with web service *SwissParam* [22-24] (www.swissparam.ch), *UCSF Chimera*® software [25], and *GROMACS*® software [26]. Hydrogens and charges were applied to the protein using the DockPrep tool in UCSF Chimera®. In *GROMACS*®, the CHARMM36 force field was used, and topology was generated in a triclinic box of 1.0 nanometers using H_2O as solvent through the TIP3P solvation method Na^+ and Cl^- (0.15 M). At the same time, ligand topologies were obtained with *SwissParam*. Employing *GROMACS*®, energy minimization for all systems was reached via the steepest descent algorithm in under 1500 steps and balances for a constant number of particles, volume, and temperature (NVT) as well as a constant number of particles, pressure, and temperature (NPT) were achieved at the temperature of 300K after a simulation of 10 nanoseconds (ns). Next, with the system assembled, the simulation was performed in 100 ns. Topology and trajectory files were retrieved after each simulation. Graphs for root mean square fluctuation (RMSF) for each atom, root mean square deviation (RMSD), radius of gyration (R_g), solvent-accessible surface area (SASA), and H-bonds were generated and plotted using *GROMACS*® and *Grace*® software, respectively, for comparison and analysis of data.

2.4 Molecular Mechanics/Poisson-Boltzmann Surface Area (MM-PBSA) calculations

To further detail the quality of binding for each ligand using estimating binding energy to their targets, Molecular Mechanics/Poisson- Boltzmann Surface Area (MM-PBSA) calculations combine

molecular mechanics (MM), which models the molecular interactions using force fields, with the Poisson-Boltzmann (PB) equation and solvent-accessible surface area (SASA) information [27]. In this study, these calculations were performed using the *gmx_MMPBSA* tool [28], an adaptation of the *MMPBSA.py* script [29], based on the trajectory files obtained after the previously described 100 ns, selecting 101 frames in intervals of 100 frames across each complex's trajectory. These frames are then used as trajectory snapshots to calculate binding free energies for the ligand and receptor separately and subsequently for the entire complex. A mean value throughout the simulation is obtained to evaluate a ligand's binding performance [29].

2.5 Literature review of chosen compounds after screening.

Furthermore, a brief review of the recent literature was performed, seeking evidence of anti-inflammatory activity for the higher-scoring compounds in molecular docking. This procedure was made using "flavonoids", "anti-inflammatory," and/or "inflammatory," as well as their common names as keywords, on the web collection of Web of Science, PubMed, and ScienceDirect.

3. Results and Discussion

3.1 Virtual screening

As described previously, the 100 flavonoids obtained previously were docked into the assigned NLRP3 structure. The following table describes data obtained for the two best-performing ligands with *GOLD*® and *BIOVIA Discovery Studio*® software [30], including RMSD values, fitness score values, and ligand-target interactions identified in the cavity.

Hence, the two compounds with the highest fitness score values, Dorsmanin C and Poinsettifolin A (Table 1), were chosen to proceed for further analysis. Both overcame the score assigned for the original inhibitor, satisfying criteria previously defined in this method for predicted biological activity. All other ligands failed to reach values near the obtained for both selected compounds and thus were not considered relevant for analysis in this study.

It can be observed that both Dorsmanin C and Poinsettifolin A bind to critical residues for activity, including Arg^{351}, Glu^{527}, and Arg^{578}, predicting binding similar to the one described for NP3-146 and providing evidence to these compound's NLRP3 inhibiting capabilities. However, it is worth noting that Poinsettifolin A makes a hydrogen bond with Arg^{578} while Dorsmanin C does not.

Table 1. Fitscore values and ligand-target interactions for both compounds.

COMPOUND	FITSCORE	INTERACTIONS					
		H-BOND	PI-CATION	PI-SIGMA	PI-PI T-SHAPED	ALKYL / PI-ALKYL	VDW
Dorsmanin C	40.35	Tyr^{443}, Ala^{228}, Asp^{662}, Tyr^{632}	Arg^{578}	Ile^{411}	Tyr^{632}	Val^{414}, Ala^{227}, Arg^{351}, Pro^{352}, Val^{353}, Ile^{574}	Met^{408}, Met^{661}, Thr^{439}, Thr^{659}, Thr^{524}, Leu^{355}, Gln^{624}, Ile^{623}, Ser^{626}, Phe^{410}, Phe^{575}, Leu^{413}, Leu^{628}, Glu^{629}, Gly^{229}, Ile^{417}
Poinsettifolin A	38.92	Asp^{662}, Tyr^{632}, Arg^{578}, Ala^{228}, Tyr^{443}	Arg^{578}	Ile^{411}	Tyr^{632}	Pro^{352}, Leu^{628}, Val^{353}, Ala^{227}	Arg^{351}, Met^{408}, Met^{661}, Thr^{439}, Thr^{659}, Thr^{524}, Phe^{410}, Phe^{575}, Ser^{658}, Ser^{626}, Leu^{413}, Gly^{229}, Gln^{225}, Gln^{624}, Glu^{369}, Glu^{629}, Ile^{574}, Val^{414}

3.2 Molecular Dynamics Simulation Analysis

The analysis of plotted parameters previously established for the protein-ligand complexes yielded notable trends. Regarding RMSD variation over time-related to complex stability (Figure 1), NLRP3 bound to Poinsettifolin A exhibited the lowest values, reaching stability at around 2 Å. It is then followed by itself bound to NP3-146, reaching stability at around 2.5 Å, the unbound protein, stabilizing at around 3 Å albeit destabilizing after 70 ns, and lastly, itself bound to Dorsmanin C, heavily destabilizing near 40 ns and displaying terrible performance. On the other hand, the ligand stability measured as RMSD variation over time (Figure 2) showed NP3-146 ranking highest, stabilizing at 0.5 Å, followed by Poinsettifolin A, stabilizing at nearly 2 Å and Dorsmanin C, not quite reaching stability with values between 1 and 3 Å.

In addition, in the RMSF per atom (Figure 3), a close trend of behavior was followed by complexes of NLRP3 with Poinsettifolin A, with NP3-146, and the unbound protein itself. Yet, Dorsmanin C could not follow the same performance as its' complex reached higher levels of fluctuation.

The stability presented by R_g data (Figure 4) had NLRP3 in complex with Poinsettifolin A as the most stable, stabilized at around 2.35 Å, over NLRP3 in complex with NP3-146, reaching stability near 2.4 Å at 60 ns, over the unbound protein, stabilizing near 2.4 Å at 20 ns, and finally over NLRP3 in complex with Dorsmanin C, heavily destabilizing after 40 ns as seen previously in complex RMSD analysis.

The number of H-bonds formed between ligands and NLRP3 across the simulations varied across complexes, with NP3-146 having the highest number, forming between 1 and 8 bonds throughout the simulation (Figure 5), followed by Poinsettifolin A, with 0 to 4 bonds formed over time (Figure 6), and Dorsmanin C which could not form more than 3 bonds at best (Figure 7).

Finally, the SASA plot (Figure 8) ranked highest for Poinsettifolin A, staying near 240 nm² until 45 ns and reaching the lowest graph values after that, followed by NP3-146 and Dorsmanin C, which abnormally did not track any more values after 25. These findings offer valuable insights into the analyzed protein-ligand complexes' relative stabilities and structural characteristics.

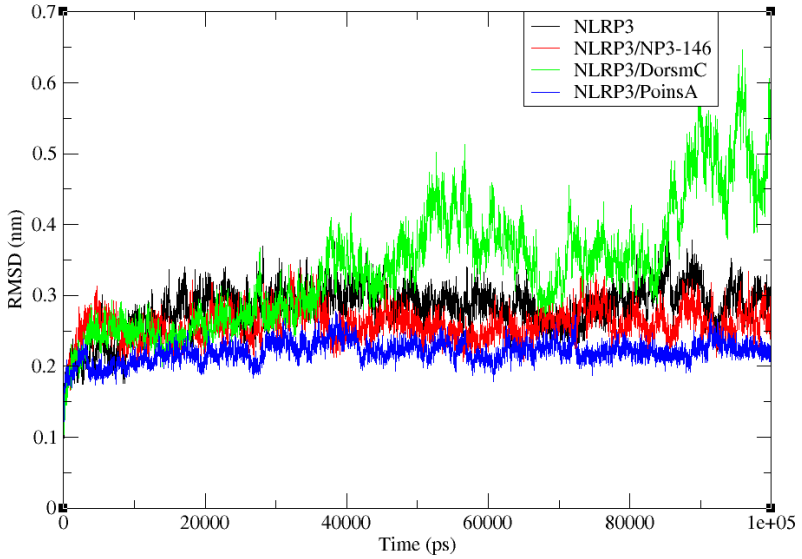

Figure 1. RMSD plot for free protein (black) and in complex with NP3-146 (red), Dorsmanin C (green), and Poinsettifolin A (blue).

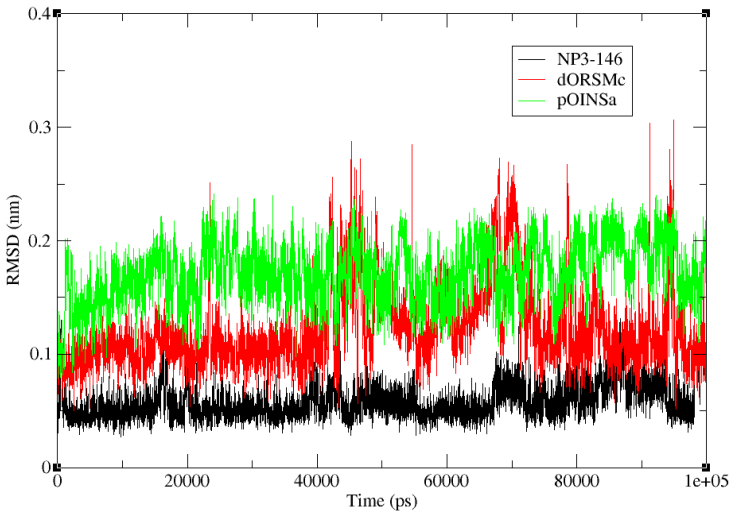

Figure 2. Ligand RMSD for NP3-146 (black), Dorsmanin C (red), and Poinsettifolin A (green).

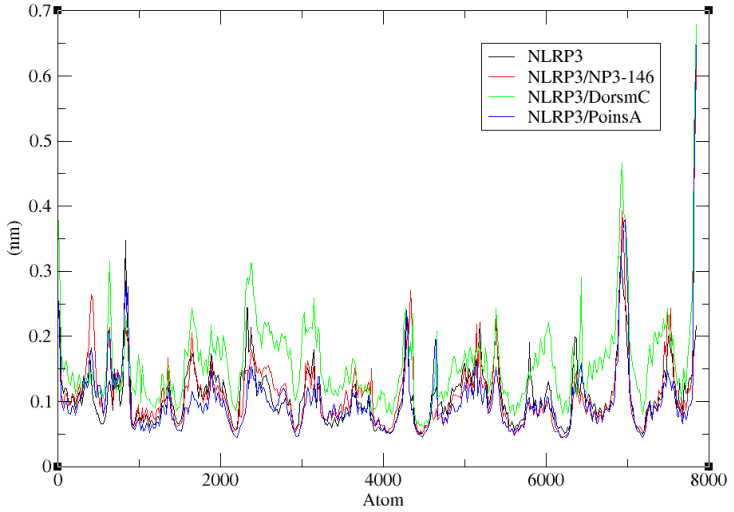

Figure 3. RMSF for each atom for the free protein (black) and in complex with NP3-146 (red), Dorsmanin C (green), and Poinsettifolin A (blue).

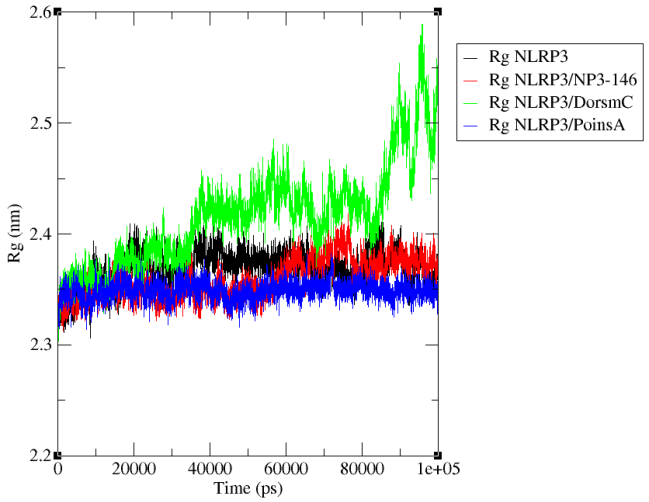

Figure 4. R_g plot for the free protein (black) and in complex with NP3-146 (red), Dorsmanin C (green), and Poinsettifolin A (blue).

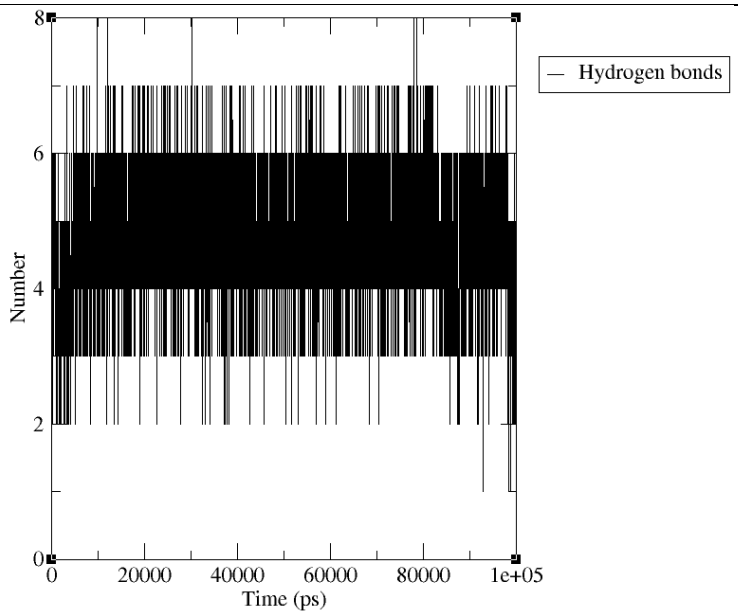

Figure 5. H-bonds plots for NP3-146.

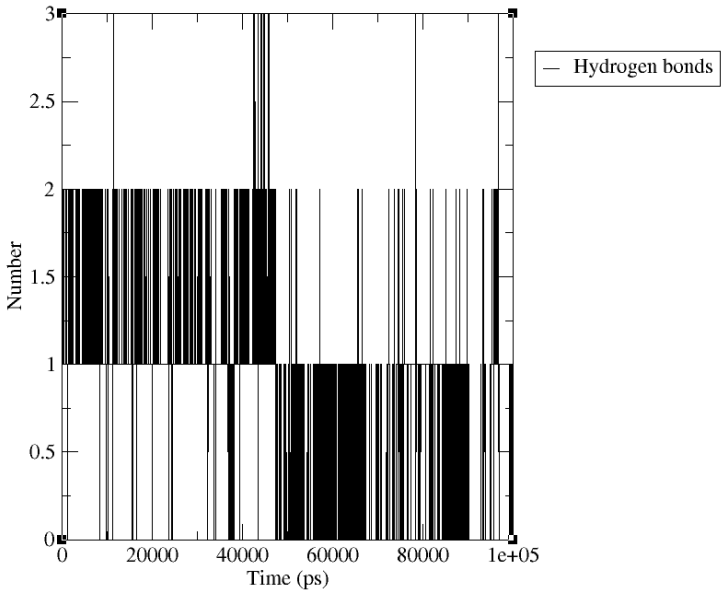

Figure 6. H-bonds plots for Dorsmanin C.

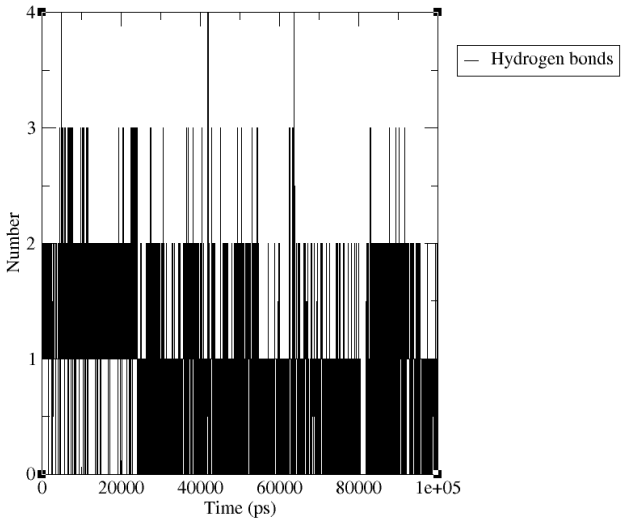

Figure 7. H-bond plot for Poinsettifolin A.

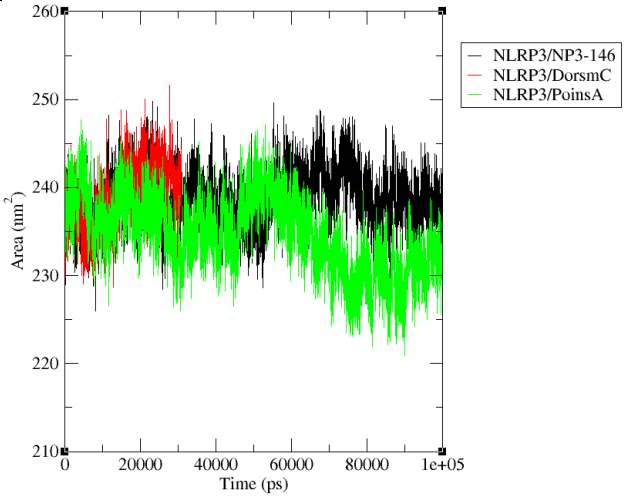

Figure 8. SASA plot for the protein complexed with NP3-146 (black), Dorsmanin C (red), and Poinsettifolin A (green).

3.3 MM/PBSA calculation

It is evident that none of the screened compounds managed to overcome NP3-146 in binding affinity, as their total average free binding energy values are well over -46.23 kcal/mol (Table 2). Despite this fact, Poinsettifolin A expectedly surpasses Dorsmanin C, maintaining its higher stability trend throughout all computational studies.

Table 2. MM/PBSA calculation results for each compound studied in MD analysis.

Compound	Binding Free Energy (kcal/mol)
Poinsettifolin A	-23.0 ± 6.34
Dorsmanin C	-16.97 ± 6.01
NP3-146	-46.23 ± 5.09

3.4 Literature review

Interestingly, the search yielded no results when inflammation-related terms were applied. Yet, when phytochemistry terms were applied, 8 articles were found about the discovery, synthesis, and characterization of Poinsettifolin A and Dorsmanin C, some showing other biological activities such as antiproliferative, antioxidant, and antimicrobial.

From what evidence could be gathered, it was found that Escobar and collaborators accomplished the first total synthesis of Poinsettifolin A, starting from commercially available materials, and biological characterization showed that it seems to be essentially non-toxic to mammalian cells [31]. Thereby, Poinsettifolin A is a promising anti-inflammatory agent of high novelty to be explored *in vivo* and *in vitro* assays, as evidence about its' anti-inflammatory activity is demonstrably sparse.

4. Conclusion

The investigation yielded noteworthy results, indicating that Dorsmanin C and Poinsettifolin A emerged as the top-performing compounds among all 100 screened flavonoids. Both compounds not

only met the screening criteria established during the validation of the docking method but also exhibited predictable binding to the crucial residue Arg^{578}, which is essential for activity.

In the MD simulations, Poinsettifolin A demonstrated a more stable binding to NLRP3 than DC and NP3-146, a recognized inhibitor of this receptor. This stability was evidenced by lower RMSD, RMSF, R_g, and SASA values evaluated for their complex.

Despite showing a relative underperformance in terms of hydrogen bonds and ligand stability compared to NP3-146, Poinsettifolin A still displayed a superior affinity to the target NLRP3 compared to Dorsmanin C. Furthermore, MM/PBSA calculations revealed a lower binding energy for NP3-146 compared to Poinsettifolin A and Dorsmanin C, emphasizing NP3-146's efficacy as an established potent inhibitor. However, Poinsettifolin A's overall superior target affinity over Dorsmanin C places it as the most promising candidate between the two.

Added to a perceived lack of yet published evidence about Poinsettifolin A’s anti-inflammatory activity, it could be inferred that this compound has potential as a lead compound for developing novel anti-inflammatory drugs, as suggested by *in silico* experiments detailed earlier. Follow-up assays of biological activity *in vitro* and *in vivo* are required to confirm this hypothesis.

ACKNOWLEDGMENTS

All authors would like to express their gratitude for the support received from the State University of Paraiba’s Graduate Studies and Research Incentive Program (PROPESQ-UEPB/Brazil), the Coordination for the Improvement of Higher Education Personnel (CAPES/Brazil), the National Council for Scientific and Technological Development (CNPq/Brazil), and the National Center for High-Performance Computing in São Paulo (CENAPAD-SP), as part of the UNICAMP/FINEP - MCTI project, for making their resources available to the development of this work.

DECLARATION OF INTEREST

All authors declare no pertinent affiliations or financial associations with any organizations or entities in financial conflicts of interest related to the subjects discussed in this manuscript, encompassing employment, consultancies, honoraria, stock ownership or options, expert testimony, grants or patents received or pending, or royalties.

REFERENCES

1. Netea, M. G.; Balkwill, F.; Chonchol, M.; Cominelli, F.; Donath, M. Y.; Giamarellos-Bourboulis, E. J.; Golenbock, D.; Gresnigt, M. S.; Heneka, M. T.; Hoffman, H. M.; Hotchkiss, R.; Joosten, L. A. B.; Kastner, D. L.; Korte, M.; Latz, E.; Libby, P.; Mandrup-Poulsen, T.; Mantovani, A.; Mills, K. H. G.; Nowak, K. L.; O’Neill, L. A.; Pickkers, P.; van der Poll, T.; Ridker, P. M.; Schalkwijk, J.; Schwartz, D. A.; Siegmund, B.; Steer, C. J.; Tilg, H.; van der Meer, J. W. M.; van de Veerdonk, F. L.; Dinarello, C. A. A Guiding Map for Inflammation. Nat. Immunol. 2017, 18 (8), 826–831. https://doi.org/10.1038/ni.3790.
2. Weavers, H.; Martin, P. The Cell Biology of Inflammation: From Common Traits to Remarkable Immunological Adaptations. J. Cell Biol. 2020, 219 (7). https://doi.org/10.1083/jcb.202004003.

3. Takeuchi, O.; Akira, S. Pattern Recognition Receptors and Inflammation. Cell 2010, 140 (6), 805–820. https://doi.org/10.1016/j.cell.2010.01.022.
4. Doyle, S.; Ozaki, E.; Campbell, M. Targeting the NLRP3 Inflammasome in Chronic Inflammatory Diseases: Current Perspectives. J. Inflamm. Res. 2015, 15. https://doi.org/10.2147/JIR.S51250.
5. Choulaki, C.; Papadaki, G.; Repa, A.; Kampouraki, E.; Kambas, K.; Ritis, K.; Bertsias, G.; Boumpas, D. T.; Sidiropoulos, P. Enhanced Activity of NLRP3 Inflammasome in Peripheral Blood Cells of Patients with Active Rheumatoid Arthritis. Arthritis Res. Ther. 2015, 17 (1), 257. https://doi.org/10.1186/s13075-015-0775-2.
6. Chi, Y. S.; Jong, H. G.; Son, K. H.; Chang, H. W.; Kang, S. S.; Kim, H. P. Effects of Naturally Occurring Prenylated Flavonoids on Enzymes Metabolizing Arachidonic Acid: Cyclooxygenases and Lipoxygenases11Abbreviations: AA, Arachidonic Acid; COX, Cyclooxygenase; LOX, Lipoxygenase; PG, Prostaglandin; TX, Thromboxane; HETE, Hydrox. Biochem. Pharmacol. 2001, 62 (9), 1185–1191. https://doi.org/10.1016/S0006-2952(01)00773-0.
7. Kim, H. P.; Son, K. H.; Chang, H. W.; Kang, S. S. Anti-Inflammatory Plant Flavonoids and Cellular Action Mechanisms. J. Pharmacol. Sci. 2004, 96 (3), 229–245. https://doi.org/10.1254/jphs.CRJ04003X.
8. Honda, H.; Nagai, Y.; Matsunaga, T.; Okamoto, N.; Watanabe, Y.; Tsuneyama, K.; Hayashi, H.; Fujii, I.; Ikutani, M.; Hirai, Y.; Muraguchi, A.; Takatsu, K. Isoliquiritigenin Is a Potent Inhibitor of NLRP3 Inflammasome Activation and Diet-Induced Adipose Tissue Inflammation. J. Leukoc. Biol. 2014, 96 (6), 1087–1100. https://doi.org/10.1189/jlb.3A0114-005RR.
9. Zhang, X.; Wang, G.; Gurley, E. C.; Zhou, H. Flavonoid Apigenin Inhibits Lipopolysaccharide-Induced Inflammatory Response through Multiple Mechanisms in Macrophages. PLoS One 2014, 9 (9), e107072. https://doi.org/10.1371/journal.pone.0107072.
10. Márquez-Flores, Y. K.; Villegas, I.; Cárdeno, A.; Rosillo, M. Á.; Alarcón-de-la-Lastra, C. Apigenin Supplementation Protects the Development of Dextran Sulfate Sodium-Induced Murine Experimental Colitis by Inhibiting Canonical and Non-Canonical Inflammasome Signaling Pathways. J. Nutr. Biochem. 2016, 30, 143–152. https://doi.org/10.1016/j.jnutbio.2015.12.002.
11. Wang, C.; Pan, Y.; Zhang, Q.-Y.; Wang, F.-M.; Kong, L.-D. Quercetin and Allopurinol Ameliorate Kidney Injury in STZ-Treated Rats with Regulation of Renal NLRP3 Inflammasome Activation and Lipid Accumulation. PLoS One 2012, 7 (6), e38285. https://doi.org/10.1371/journal.pone.0038285.
12. Wu, J.; Xu, X.; Li, Y.; Kou, J.; Huang, F.; Liu, B.; Liu, K. Quercetin, Luteolin and Epigallocatechin Gallate Alleviate TXNIP and NLRP3-Mediated Inflammation and Apoptosis with Regulation of AMPK in Endothelial Cells. Eur. J. Pharmacol. 2014, 745, 59–68. https://doi.org/10.1016/j.ejphar.2014.09.046.
13. dos Santos Nascimento, I. J.; da Silva-Júnior, E. F. TNF-α Inhibitors from Natural Compounds: An Overview, CADD Approaches, and Their Exploration for Anti-Inflammatory Agents. Comb. Chem. High Throughput Screen. 2021, 24. https://doi.org/10.2174/1386207324666210715165943.
14. Nascimento, I. J. dos S.; de Aquino, T. M.; da Silva-Júnior, E. F. The New Era of Drug Discovery: The Power of Computer-Aided Drug Design (CADD). Lett. Drug Des. Discov. 2022, 19 (11), 951–955. https://doi.org/10.2174/1570180819666220405225817.
15. Irwin, J. J.; Tang, K. G.; Young, J.; Dandarchuluun, C.; Wong, B. R.; Khurelbaatar, M.; Moroz, Y. S.; Mayfield, J.; Sayle, R. A. ZINC20 - A Free Ultralarge-Scale Chemical Database for Ligand Discovery. J Chem Inf Model 2020, 60 (12), 6065–6073. https://doi.org/10.1021/acs.jcim.0c00675.

16. Jiménez-Avalos, G.; Vargas-Ruiz, A. P.; Delgado-Pease, N. E.; Olivos-Ramirez, G. E.; Sheen, P.; Fernández-Díaz, M.; Quiliano, M.; Zimic, M.; Agurto-Arteaga, A.; Antiparra, R.; Ardiles-Reyes, M.; Calderon, K.; Cauna-Orocollo, Y.; de Grecia Cauti-Mendoza, M.; Chipana-Flores, N.; Choque-Guevara, R.; Chunga-Girón, X.; Criollo-Orozco, M.; De La Cruz, L.; Delgado-Ccancce, E.; Elugo-Guevara, C.; Fernández-Sanchez, M.; Guevara-Sarmiento, L.; Gutiérrez, K.; Heredia-Almeyda, O.; Huaccachi-Gonzalez, E.; Huerta-Roque, P.; Icochea, E.; Isasi-Rivas, G.; Juscamaita-Bartra, R. A.; Licla-Inca, A.; Montalvan, A.; Montesinos-Millan, R.; Núñez-Fernández, D.; Ochoa-Ortiz, A.; Páucar-Montoro, E.; Pauyac, K.; Perez-Martinez, J. L.; Perez-M, N.; Poma-Acevedo, A.; Quiñones-Garcia, S.; Ramirez-Ortiz, I.; Ramos-Sono, D.; Rios-Angulo, A. A.; Rios-Matos, D.; Rojas-Neyra, A.; Romero, Y. K.; Salguedo-Bohorquez, M. I.; Sernaque-Aguilar, Y.; Soto, L. F.; Tataje-Lavanda, L.; Ticona, J.; Vallejos-Sánchez, K.; Villanueva-Pérez, D.; Ygnacio-Aguirre, F. Comprehensive Virtual Screening of 4.8 k Flavonoids Reveals Novel Insights into Allosteric Inhibition of SARS-CoV-2 MPRO. Sci Rep 2021, 11 (1), 1–19. https://doi.org/10.1038/s41598-021-94951-6.
17. Thompson, M.A. (2004) Molecular Docking Using ArgusLab, an Efficient Shape-Based Search Algorithm and the a Score Scoring Function. ACS Meeting, Philadelphia.
18. Bateman, A.; Martin, M.-J.; Orchard, S.; Magrane, M.; Ahmad, S.; Alpi, E.; Bowler-Barnett, E. H.; Britto, R.; Bye-A-Jee, H.; Cukura, A.; Denny, P.; Dogan, T.; Ebenezer, T.; Fan, J.; Garmiri, P.; da Costa Gonzales, L. J.; Hatton-Ellis, E.; Hussein, A.; Ignatchenko, A.; Insana, G.; Ishtiaq, R.; Joshi, V.; Jyothi, D.; Kandasaamy, S.; Lock, A.; Luciani, A.; Lugaric, M.; Luo, J.; Lussi, Y.; MacDougall, A.; Madeira, F.; Mahmoudy, M.; Mishra, A.; Moulang, K.; Nightingale, A.; Pundir, S.; Qi, G.; Raj, S.; Raposo, P.; Rice, D. L.; Saidi, R.; Santos, R.; Speretta, E.; Stephenson, J.; Totoo, P.; Turner, E.; Tyagi, N.; Vasudev, P.; Warner, K.; Watkins, X.; Zaru, R.; Zellner, H.; Bridge, A. J.; Aimo, L.; Argoud-Puy, G.; Auchincloss, A. H.; Axelsen, K. B.; Bansal, P.; Baratin, D.; Batista Neto, T. M.; Blatter, M.-C.; Bolleman, J. T.; Boutet, E.; Breuza, L.; Gil, B. C.; Casals-Casas, C.; Echioukh, K. C.; Coudert, E.; Cuche, B.; de Castro, E.; Estreicher, A.; Famiglietti, M. L.; Feuermann, M.; Gasteiger, E.; Gaudet, P.; Gehant, S.; Gerritsen, V.; Gos, A.; Gruaz, N.; Hulo, C.; Hyka-Nouspikel, N.; Jungo, F.; Kerhornou, A.; Le Mercier, P.; Lieberherr, D.; Masson, P.; Morgat, A.; Muthukrishnan, V.; Paesano, S.; Pedruzzi, I.; Pilbout, S.; Pourcel, L.; Poux, S.; Pozzato, M.; Pruess, M.; Redaschi, N.; Rivoire, C.; Sigrist, C. J. A.; Sonesson, K.; Sundaram, S.; Wu, C. H.; Arighi, C. N.; Arminski, L.; Chen, C.; Chen, Y.; Huang, H.; Laiho, K.; McGarvey, P.; Natale, D. A.; Ross, K.; Vinayaka, C. R.; Wang, Q.; Wang, Y.; Zhang, J. UniProt: The Universal Protein Knowledgebase in 2023. Nucleic Acids Res 2023, 51 (D1), D523–D531. https://doi.org/10.1093/nar/gkac1052.
19. Berman, H. M. The Protein Data Bank. Nucleic Acids Res 2000, 28 (1), 235–242. https://doi.org/10.1093/nar/28.1.235.
20. Dekker, C.; Mattes, H.; Wright, M.; Boettcher, A.; Hinniger, A.; Hughes, N.; Kapps-Fouthier, S.; Eder, J.; Erbel, P.; Stiefl, N.; Mackay, A.; Farady, C. J. Crystal Structure of NLRP3 NACHT Domain With an Inhibitor Defines Mechanism of Inflammasome Inhibition. J Mol Biol 2021, 433 (24). https://doi.org/10.1016/j.jmb.2021.167309.
21. Verdonk, M. L.; Cole, J. C.; Hartshorn, M. J.; Murray, C. W.; Taylor, R. D. Improved Protein-Ligand Docking Using GOLD. Proteins: Structure, Function, and Bioinformatics 2003, 52 (4), 609–623. https://doi.org/10.1002/prot.10465.

22. Yesselman, J. D.; Price, D. J.; Knight, J. L.; Brooks, C. L. MATCH: An Atom-typing Toolset for Molecular Mechanics Force Fields. J Comput Chem 2012, 33 (2), 189–202. https://doi.org/10.1002/jcc.21963.
23. Zoete, V.; Cuendet, M. A.; Grosdidier, A.; Michielin, O. SwissParam: A Fast Force Field Generation Tool for Small Organic Molecules. J Comput Chem 2011, 32 (11), 2359–2368. https://doi.org/10.1002/jcc.21816.
24. Bugnon, M.; Goullieux, M.; Röhrig, U. F.; Perez, M. A. S.; Daina, A.; Michielin, O.; Zoete, V. SwissParam 2023: A Modern Web-Based Tool for Efficient Small Molecule Parametrization. J Chem Inf Model 2023, 63 (21), 6469–6475. https://doi.org/10.1021/acs.jcim.3c01053.
25. Pettersen, E. F.; Goddard, T. D.; Huang, C. C.; Couch, G. S.; Greenblatt, D. M.; Meng, E. C.; Ferrin, T. E. UCSF Chimera—A Visualization System for Exploratory Research and Analysis. J Comput Chem 2004, 25 (13), 1605–1612. https://doi.org/10.1002/jcc.20084.
26. Abraham, M. J.; Murtola, T.; Schulz, R.; Páll, S.; Smith, J. C.; Hess, B.; Lindahl, E. GROMACS: High Performance Molecular Simulations through Multi-Level Parallelism from Laptops to Supercomputers. SoftwareX 2015, 1–2, 19–25. https://doi.org/10.1016/j.softx.2015.06.001.
27. Genheden, S.; Ryde, U. The MM/PBSA and MM/GBSA Methods to Estimate Ligand-Binding Affinities. Expert Opinion on Drug Discovery. Informa Healthcare May 1, 2015, pp 449–461. https://doi.org/10.1517/17460441.2015.1032936.
28. Valdés-Tresanco, M. S.; Valdés-Tresanco, M. E.; Valiente, P. A.; Moreno, E. Gmx_MMPBSA: A New Tool to Perform End-State Free Energy Calculations with GROMACS. J Chem Theory Comput 2021, 17 (10), 6281–6291. https://doi.org/10.1021/acs.jctc.1c00645.
29. Miller, B. R.; McGee, T. D.; Swails, J. M.; Homeyer, N.; Gohlke, H.; Roitberg, A. E. MMPBSA.Py: An Efficient Program for End-State Free Energy Calculations. J Chem Theory Comput 2012, 8 (9), 3314–3321. https://doi.org/10.1021/ct300418h.
30. BIOVIA Dassault Systèmes. Discovery Studio Visualizer. BIOVIA, Dassault Systèmes: San Diego 2023.
31. Escobar, Z.; Solano, C.; Larsson, R.; Johansson, M.; Salamanca, E.; Gimenez, A.; Muñoz, E.; Sterner, O. Synthesis of Poinsettifolin A. Tetrahedron 2014, 70 (47), 9052–9056. https://doi.org/10.1016/j.tet.2014.10.021.